The 2022 International Future Energy Challenge

University of Moratuwa

Smart, Efficient and Light Solar Microgrid Inverter

Authors:

Mendis N.P.A., Somarathne P.M.P.H., Wijitharathna K.M.R., Mahawela P.D.,

Mudalige D.N., Witharama W.M.N., Wijegunawardana C.H.W., Wijewardena L.H.N.

Supervisors:

Prof.Udayanga Hemapala

Head of Department,

Dept. of Electrical Engineering,

University of Moratuwa

Mr. Thilina Ambagahawaththa

Lecturer,

Dept. of Electronic and Telecommunication

Engineering,

University of Moratuwa

Mr. Iresh Jayawardana

Graduate,

Dept. of Electronic and Telecommunication

Engineering,

University of Moratuwa

October 27, 2021

Contents

List of Figures

List of Tables

List of Abbreviations

AC Alternating Current. i, 4

ADC Analog to Digital Converter. 10

DC Direct Current. i, 2–5

GaN Gallium Nitride. 3

INC Incremental Conductance. 2, 3

IO Input Output. 10

MCU Microcontroller Unit. 10

MPPT Maximum Power Point Tracking. i, ii, 2–4, 7, 8, 11

PI Proportional Integral. 3, 6

PLL Phase Locked Loop. 6

PV Photo Voltaic. 1, 3, 4, 7, 11

PWM Pulse Width Modulation. 3, 5, 10

SiC Silicon Carbide. 3, 10

SPWM Sinusoidal Pulse Width Modulation. 3

SVPWM Space Vector Pulse Width Modulation. 3, 5, 6

THD Total Harmonic Distortion. ii, 2, 3, 9

VSI Voltage Source Inverter. i, 4, 5

WBG Wide Band Gap. 2, 3, 10

1 Introduction

Renewable energy is defined as energy derived from natural resources that can regenerate within a human lifetime. It has seen immense growth during the past few decades. There are many reasons behind the rapid popularity and advancement [6].

- Capability to replace environmentally endangering energy sources such as fossil fuel
- Increase in technological advancements
- Increase in the price of non-renewable energy sources

Therefore, many governments have initiated necessary planning to adapt renewable energy into the national grid distribution. Specifically, PV energy is being encouraged to be established on a small scale throughout countries to supply energy to isolated areas as well as to contribute to the grid. Implementation of PV microgrid systems offers many advantages to both the user and the electric utility provider. The application of a microgrid that is connected to a grid can improve network quality, reduce the energy loss, improve the emission, and reduce the cost incurred by the user as the electric utility provider can reduce power flow on lines of transmission and distribution by consequently reducing losses and costs for network development. Microgrids can also decrease the load of the grid to meet the electricity demand and help to support the grid locally if a fault occurs. Addressing the above important cause, this proposal presents a cost effective, efficient and smart microgrid inverter for 2022 International Future Energy Challenge. Table 1 shows the specifications of our inverter design. Furthermore, the inverter will feature maximum power point tracking to obtain the highest power efficiency from the PV arrays.

Table 1: Specifications

Input Voltage	36V-60V DC (48V nominal)
Input Current	Limited to 20A DC with ripple <10%
Output Voltage	Single Phase - 120∼230V AC Three Phase - 208∼260V AC
Grid Frequency	40-65 Hz
Output Power	Maximum of 1 kW
Total Harmonic Distortion	<2% at 1 kW
Power Factor	>0.99 at 1kW active power
Efficiency	>95% at 1kW / >94% at 500W

2 Literature Review

The main components of a microgrid inverter can be identified as follows [14].

- MPPT
- Boost Converter
- Inverter

There are several approaches used in the implementation of MPPT.MPPT algorithm dynamically adjusts the voltage to ensure power optimization to achieve sustainable efficiency [15]. There are two widely used direct methods in the implementation of MPPT.

- Perturb and Observe
- Incremental Conductance (INC)

Apart from that, there are methods like fixed voltage and fractional open circuit voltage methods offering very simple calculations but the direct methods provide more accurate tracking.Direct methods also guarantee a higher energy conversion efficiency and do not need periodical tuning of the parameter [2]. In the Perturb and Observe Method, the power is tracked continuously. It suffers from oscillation and the step size determines both the accuracy and tracking time. In the INC method, oscillation under certain conditions can occur. The efficiency depends on the level of disturbance in both methods [9]. There are two approaches that can be used as Boost Converters namely synchronous and non-synchronous. A non-synchronous topology is an older design, noted for power loss across the external Schottky diode. A synchronous topology is recommended here because it offers high efficiency and fits in a more compact form factor by integrating an efficient MOSFET [7]. There are various topologies that can be considered in implementing the inverter as shown in Table 2.

Table 2: Inverter Topologies

Topology	Advantages	Disadvantages
2 Level H Bridge [5]	Simpler Design Lower number of components	Lower Efficiency Higher THD
Multilevel Cascaded H Bridge [5]	Higher Efficiency Lower THD	Higher number of components Multiple DC sources
Flying Capacitor [12]	Phase Redundancy	Bulky in size
Impedance Source Inverter [1]	Boosting capability	Complex Control

There are various types of components that can be used as switching elements.WBGdevices replace Si semiconductors. The advantages of using WBG devices are the ability to operate in higher temperature

levels, higher breakdown voltages, lower conduction losses, higher power density and higher switching frequency. Most WBG devices are based on either GaN or SiC. The GaN devices are suitable for voltage and current levels up to 600 V and 30 A respectively,low power and high frequency switching circuits.SiC devices are preferred discrete devices with breakdown voltages up to 1.7 kV and current up to 100 A [13]. The most common types of control for two-level voltage source inverter are SPWM and SVPWM. SVPWM achieves better control of THD while increasing input voltage capabilities [16]. There are also several controller schemes involved in the design such as PI controller which allows for a simpler design [8].

3 Proposed Methodology

3.1 Block Diagram

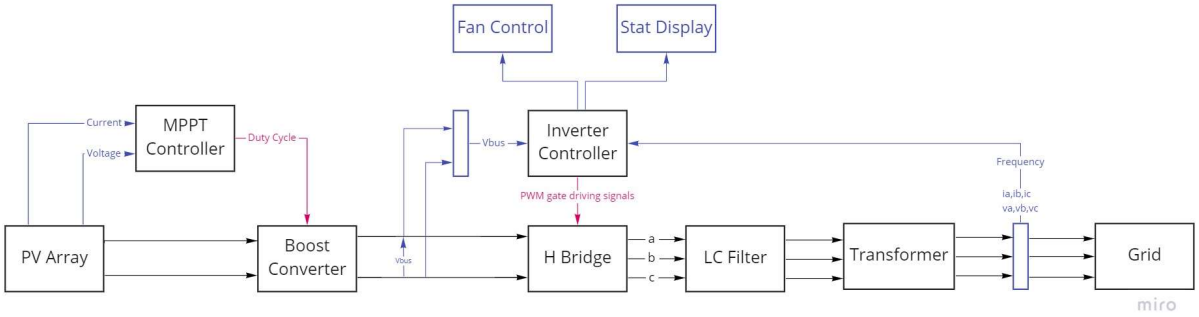

Figure 1: Block Diagram

3.2 MPPT Controller

Incremental conductance algorithm which is implemented inside the controller, requires measurements of output voltage and current of the PV module as inputs. Figure 2 shows the flow chart of the *INC Algorithm* which has been implemented in the simulation. The generated PWM signal from the MPPT is used to control the converter in the DC-DC stage.

3.3 DC-DC Conversion - Boost Converter

The boost converter in the DC-DC stage steps up the voltage from the PV array according to the control signal given by the MPPT. Maximum input voltage to the DC-DC converter is 60V. This DC – DC conversion stage is consistent with two functionalities.

- Allows Maximum Power Point Tracking (MPPT) : The booster changes its input impedance in a way such that it draws the maximum power from the PV module.

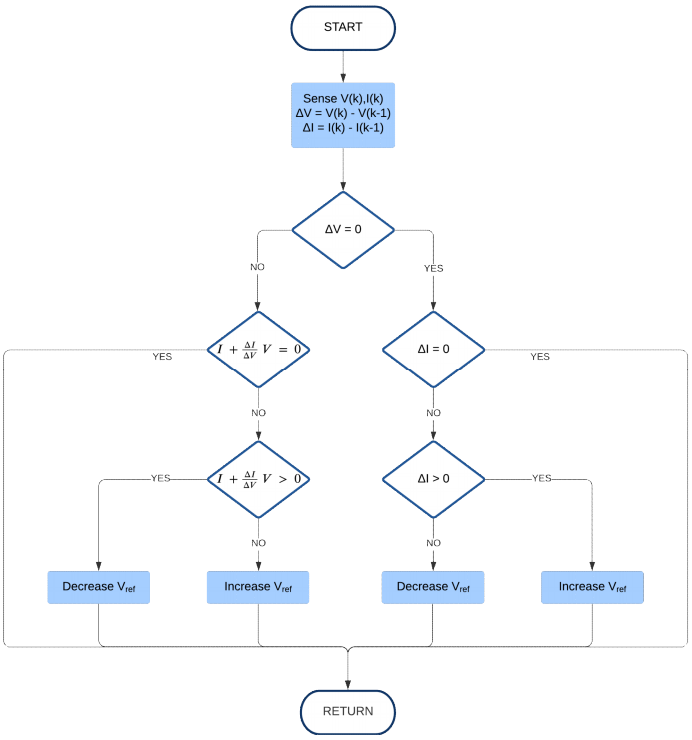

Figure 2: MPPT Algorithm

- Steps up the voltage : The boost converter steps up the voltage obtained from the PV array. However, this voltage may vary with time. This is fed into the DC- AC converter.

The synchronous boost converter is selected as it enables stepping up of the voltage to the required level for the DC-AC stage while enabling the desired efficiency.

3.4 DC-AC Conversion - Inverter

The inverter receives the voltage of the boost converter as its input and generates 3-phase AC waveforms using a *3-phase two-level* voltage-source converter topology. This is a commonly used topology in low-power PV microgrid inverter systems [4]. The advantage of using this topology is its simplicity in implementation and controlling. The 3-phase VSI consists of *6 bi-directional switching transistors* arranged into 3 legs of two transistors each. The low number of components used in the inverter topology enables our design to have a higher power density, increases the efficiency and reduces the cost. Also, as the conduction and switching losses are reduced, the requirement of heat sinks are reduced,making the inverter lighter and smaller. All three legs are connected across two capacitors on the DC side which creates the two voltage levels. The capacitance of the two capacitors is large which makes the DC voltage nearly constant. Each of the three phases are drawn from the middle of each leg. When the inverter is

operating in single phase mode, one leg is disabled and the live and neutral wires are drawn from the middle of the remaining two legs.

The switches are controlled using 6 pulse width modulated (PWM) signals generated from the controller. The two switching signals for transistors of each leg are complements of each other, which reduces the complexity of the design.The PWM waves include a deadtime to avoid the complementary switches being switched on simultaneously. They are connected to the switching elements through a gate driver.

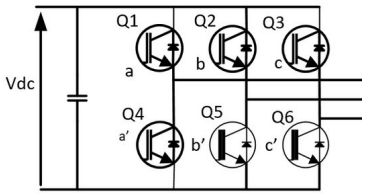

Figure 3: Two Level VSI

3.5 Filtering - Band-Pass LCL Filter

Since the output of the inverter consists of odd harmonics of the waveform a band pass filter is used to reduce total harmonic distortion. As shown in the bode plot in Figure 5 *a third order LCL filter* satisfies the requirement of attenuating the harmonics signals (90dB attenuation at 180Hz). When choosing the values of the components the capacitance is chosen to minimize the reactive power generation.

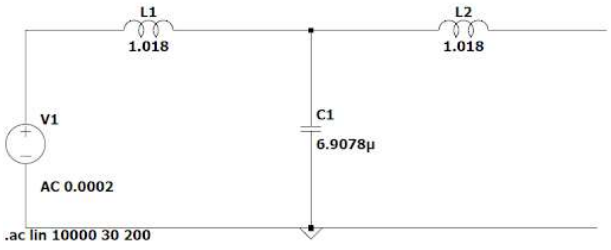

Figure 4: LCL Filter

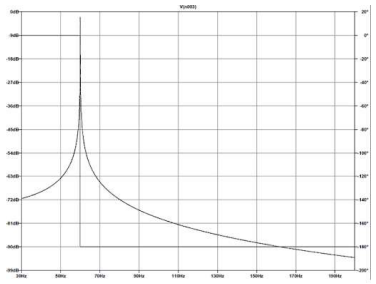

Figure 5: Response

3.6 Controller

The controller is responsible for generating the signals to drive the transistors, while adhering to the specification given in Table 1. SVPWM scheme is used to determine the switching times. Apart from that, the controller also maintains the DC link voltage at the desired level and controls whether the

system generates active power or reactive power. The controller comprises of components shown in the Figure 6.

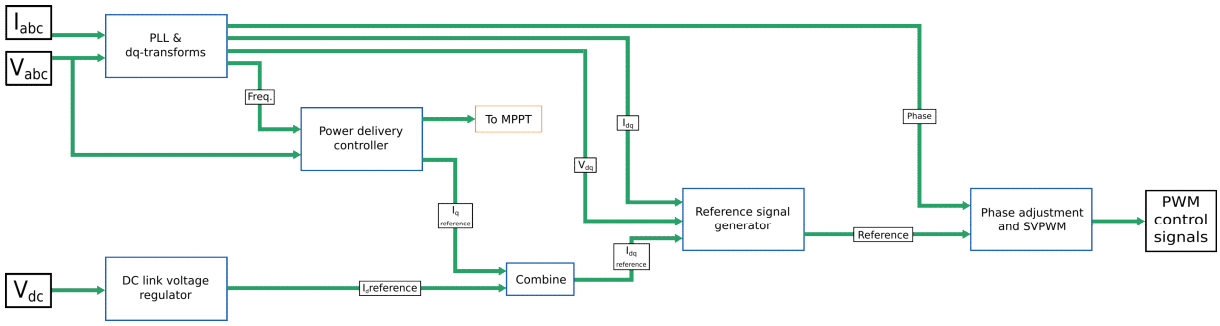

Figure 6: Controller Block Diagram

The PLL is responsible for determining the phase and frequency signals from the grid. The voltage regulator uses a PI controller to generate the current output to maintain the DC link voltage at a desired value. Power delivery controller is responsible for frequency and voltage based droop control according to the given specifications. Reference signal generator comprises several stages. A PI controller is used to control the current. Active and reactive voltages are controlled with respect to the current reference using a proportional controller. The output of the reference generator is phase adjusted to compensate for timing delays and reactive component effects before being converted to SVPWM signals at 20 kHz frequency.

3.7 Cooling

Several solutions to avoid heating of the inverter system are proposed. A temperature sensors is used to measure the temperature around the inverter H bridge, where most of the power dissipation happens. Heatsinks of the necessary size are added around the switching transistors and other components,based on the hardware test results of these temperature sensors. A forced cooling method, such as a fan, is also implemented depending on the cooling requirement measured in the hardware implementation. This is controlled by the microcontroller according to conditions defined based on the testing results.

3.8 Protection Methods

The protection methods those are implemented in our design are as follows.

- Short Circuit Protection
- Over Current Protection
- Over Voltage Protection
- Over Temperature Protection

The wires of the system will be isolated from the frame to avoid leakage. To avoid arm short protection,

a deadtime is added to the gate control signals of the transistors. The gate driver is chosen to provide short circuit protection.Over voltage and current protection is managed by the controller which monitors the input and output voltages and currents and shuts down the inverter in case such fault happens. The temperature sensors that are used for cooling purposes sends the temperature measurements to the controller. The controller shuts down the inverter if the temperature exceeds a pre-determined temperature value. The transformer in our design will provide galvanic isolation between the inverter and the grid.

4 Simulations and Results

The following simulation diagram is realized on Simulink 2021a to verify our design. The PV array and the grid are modelled according to the specifications.The Figure 8 shows the outputs obtained by the simulation schematic shown in the Figure 7. Due to the initialization, the results shown in the Figure 8 is not stabilized until 0.5s. The first waveform in the Figure 8a shows the voltage and the second waveform shows the current of a single phase. The Figure 8c shows the operation of the MPPT. The blue waveform shows the maximum power while the yellow waveform shows the power drawn from the PV array. The performance of the proposed implementation can further be improved by fine-tuning the parameters of the controller.

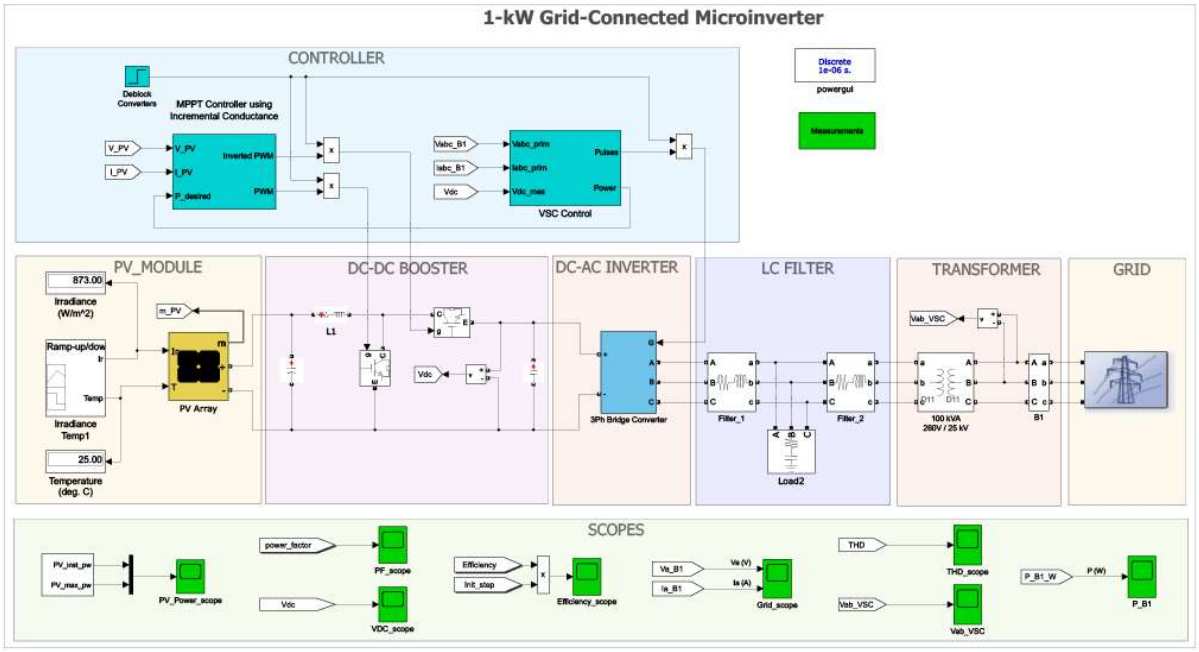

Figure 7: Simulation Schematic

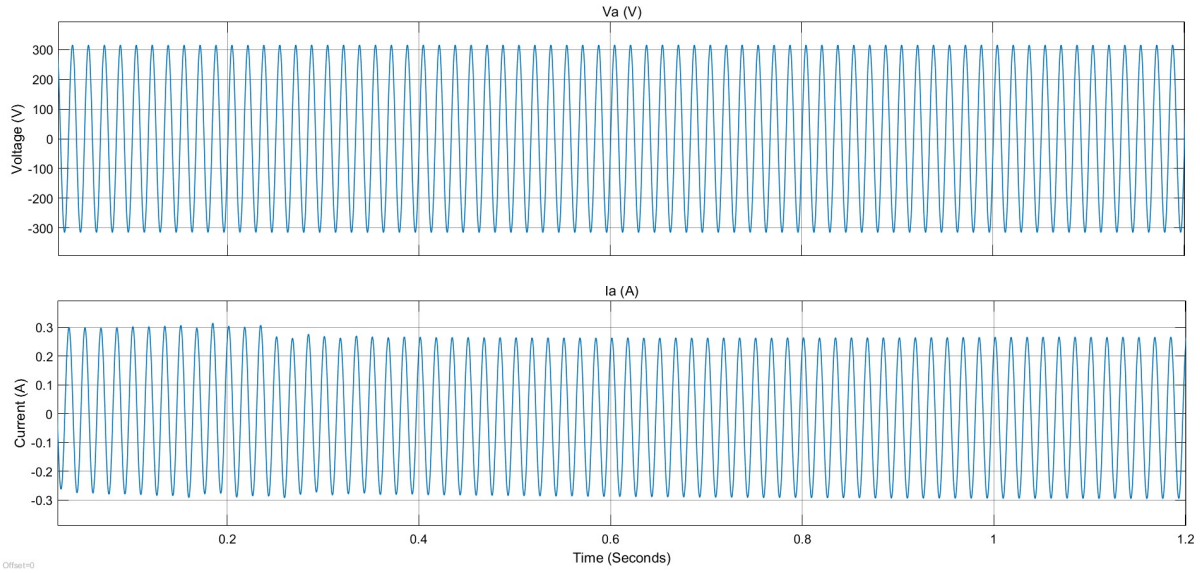

(a) Output side phase-to-phase voltage (Top) and phase-to-phase current (Bottom) of phase-a

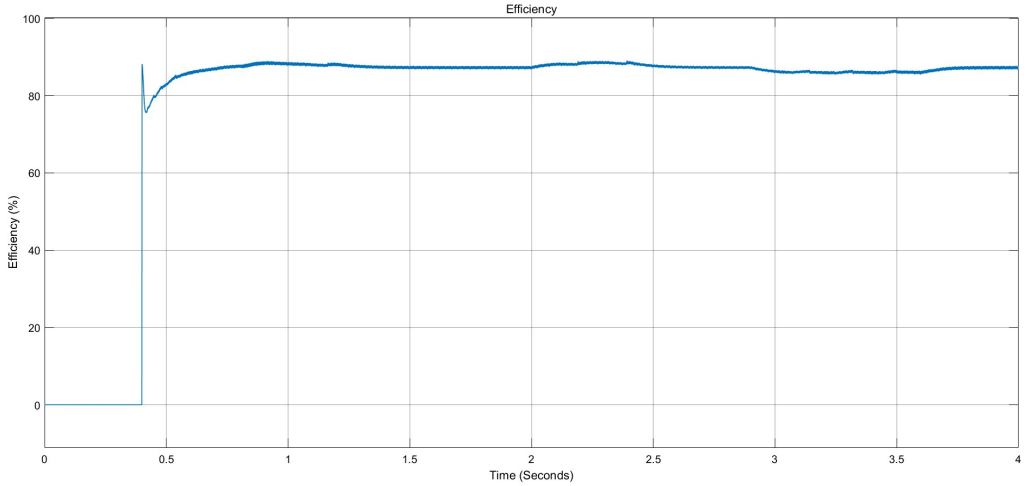

(b) Efficiency (%)

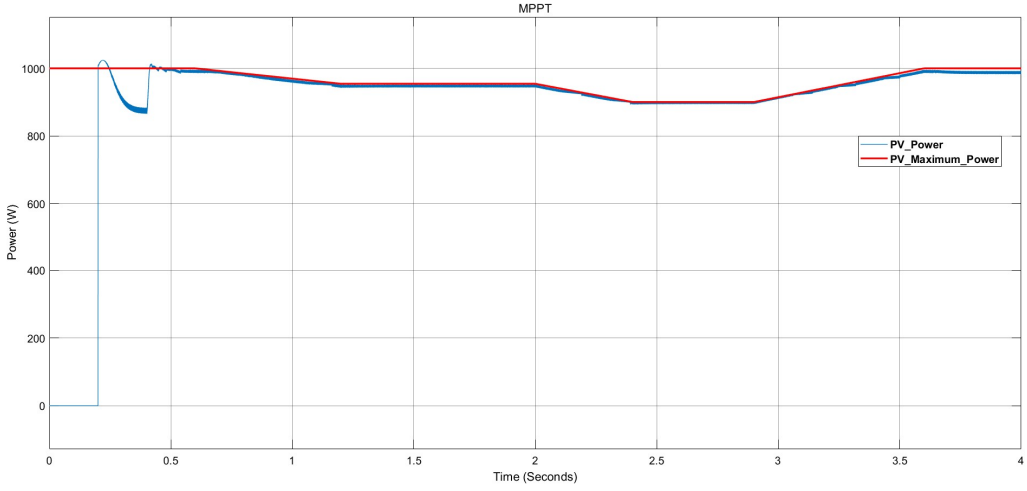

(c) MPPT operation: Tracking the maximum power point during irradiance change

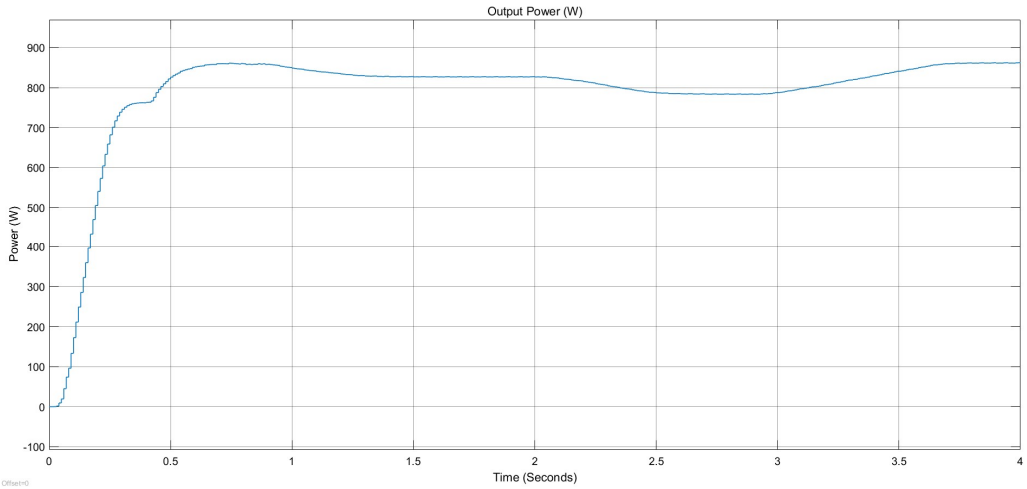

(d) Output Power

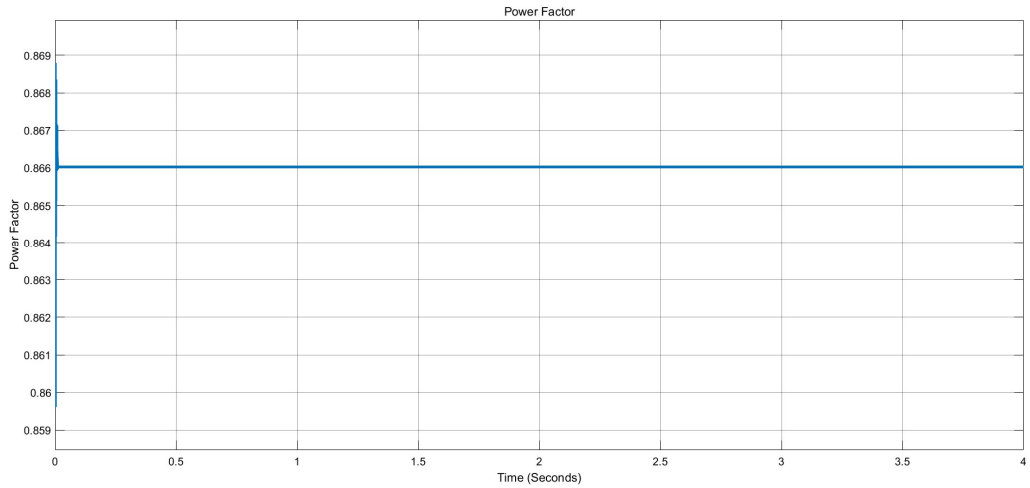

(e) Power Factor

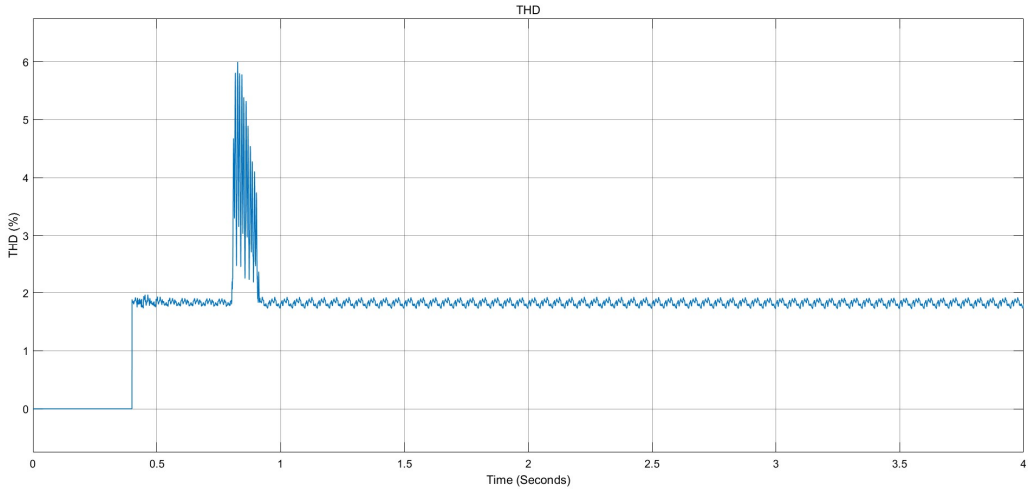

(f) THD

Figure 8: Simulation Results

5 Component Selection and Cost

SiC wide band-gap devices are used as our switching elements. By using wide band gap transistors,a high switching frequency to lower the total harmonic distortion is used. The on resistance is low in WBG devices and the conduction losses can be diminished.The UJ4C075033K3S from UnitedSiC is selected, as it can handle 750V blocking voltage and 47A drain current [17], which are 8 and 4 times of the needed values respectively. As the gate driver, ZXGD3006E6 from Diodes Inc. is selected as it can switch in less than 50ns and can supply upto 10A drive current [10] (10x than needed). This gate driver also features short circuit protection. TMS320F28384D from Texas Instruments is selected as the MCU as it has two cores that can work in parallel to control inverter-side and booster-side independently [11]. It also has an abundance of IO options for measurements, (ADC) and control signals (PWM). This MCU is perfectly capable of delivering the computational power needed for this inverter. The cost of an enclosure with cooling is estimated to be $10 at most. The total breakdown of major cost components are as illustrated in Figure 9 in Appendix 1.

6 Project Deliverables and Timeline

At the end of the completion of the project,a complete working prototype will be presented as a proof of concept.This target will be achieved before the deadline specified by the competition guidelines. The inverter prototype will be completed with a suitable enclosure and will be shipped for testing as required. The timeline in the Appendix 2 is followed to complete the above deliverables adhering to the deadlines.

7 Lifetime Analysis

The inverter is expected to have lifetime of more than 10 years with minimum maintenance. Therefore, the components in the main power path and the controllers are considered to be the most critical in the lifetime analysis.The components with the highest possible lifetime with low maintenance cost is selected while satisfying the required specifications. The enclosure is manufactured by injection molding using a durable material as well in large scale production. After the final design implementation,a proper lifetime analysis is conducted based on the test results to provide a verified life expectancy [3].

8 Conclusion

This report presents the proposal of a smart, efficient and light solar microgrid inverter for International Future Energy Challenge 2022. A design of a microgrid inverter that has the ability to provide the required grid voltages in both single phase and three phase modes is proposed.Wide band gap semiconductor devices are used to implement the switching elements. The inverter controller tracks the fluctuations in the grid voltage and frequency and adjust the inverter parameters to supply a compatible voltage to the grid. The MPPT controller that is implemented draws maximum power from the PV array whenever possible while abiding to the active power delivery curve specified by the request of a proposal. Furthermore, the inverter features several protection methods like short circuit protection, overcurrent protection, over voltage protection and over temperature protection.

Appendix 1

Component	Manufacturer	Manufacturer Part Number	Unit Price	Quantity	Total
MOSFET switch	UnitedSiC	UJ4C075033K3S	$7.00	8	$56.00
Gate driver	Diodes incorporated	ZXGD3006E6	$0.25	8	$2.00
Microcontroller	Texas Instruments	TMS320F28384D	$10.60	1	$10.60
Current and voltage sensors	Texas Instruments	AMC1350 + TMCS1100	$7.25	3	$21.75
PCB/Assembly	JLCPCB	4 layer, 20x20cm, + assembly	$15.00	1	$15.00
Boost controller inductor	Wurth	74436410470	$4.87	1	$4.87
Filter capacitors	KEMET	C4AQLBW6100M3MK	$8.00	3	$24.00
FIlter inductors	Bourns	2200LL-560-V-RC	$2.58	6	$15.48
Boost controller output cap	Cornell Dubilier Electronics (CDE)	383LX123M100N082	$9.11	1	$9.11
Passive components			$8.00	1	$8.00
Inverter transformer	Custom Manufacturing	Core+Windings	$25.00	1	$25.00
Enclosure & heatsinks			$8.00	1	$8.00
					$199.81

Figure 9: Proposed cost

Appendix 2

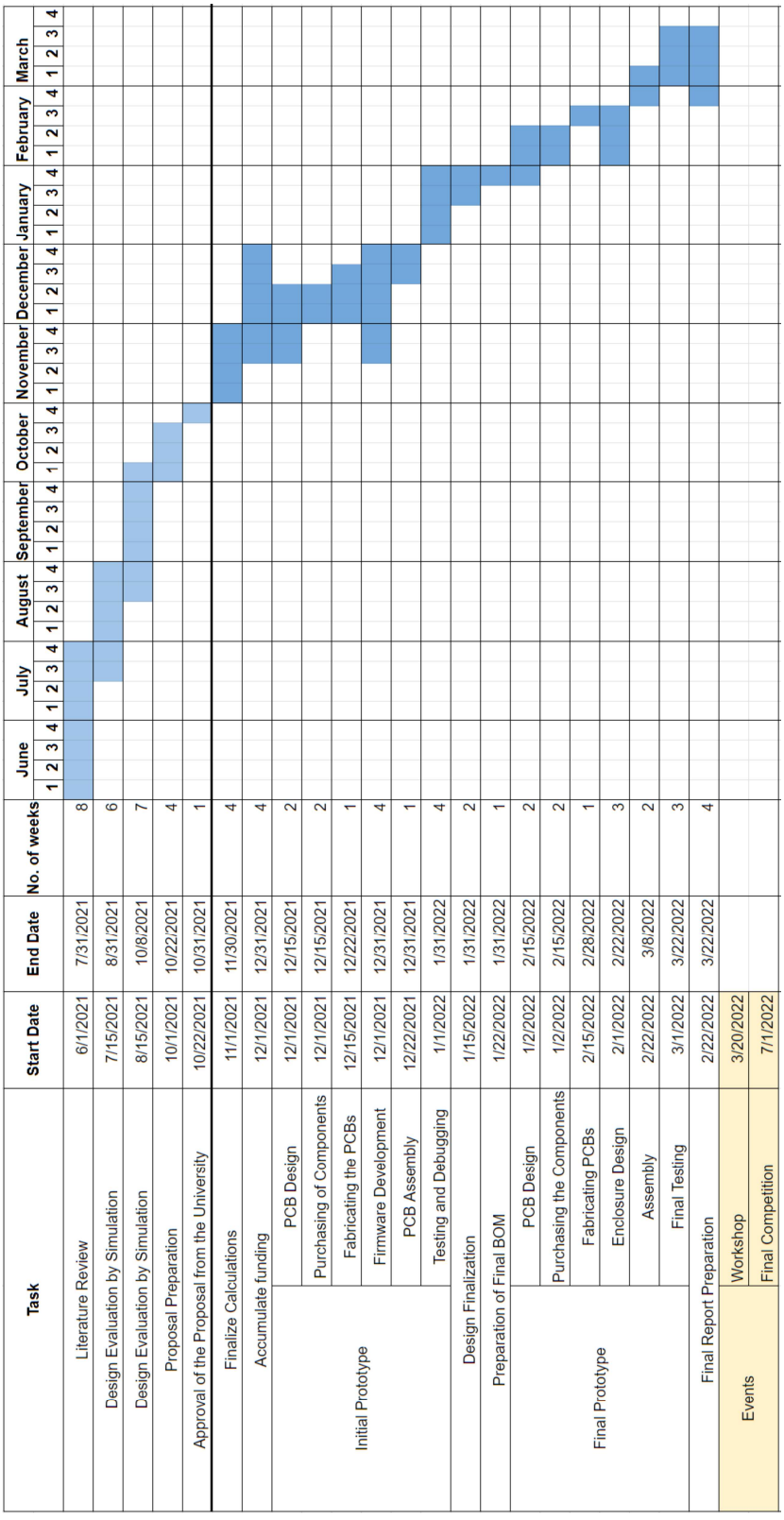

Figure 10: Proposed Timeline

References

[1] Haitham Abu-Rub, Mariusz Malinowski, and Kamal Al-Haddad. "Impedance Source Inverters". In: *Power Electronics for Renewable Energy Systems, Transportation and Industrial Applications*. IEEE, 2014, pp. 766–785. ISBN: 9781118755518. DOI: 10.1002/9781118755525.ch24. URL: https://ieeexplore.ieee.org/document/7794201 (visited on 10/26/2021).

[2] Ali Omar Baba, Guangyu Liu, and Xiaohui Chen. "Classification and Evaluation Review of Maximum Power Point Tracking Methods". en. In: *Sustainable Futures* 2 (Jan. 2020), p. 100020. ISSN: 2666-1888. DOI: 10.1016/j.sftr.2020.100020. URL: https://www.sciencedirect.com/science/article/pii/S2666188820300137 (visited on 10/26/2021).

[3] Carmelo Barbagallo et al. *On the lifetime estimation of SIC power mosfets for motor drive applications*. Jan. 2021. URL: https://www.mdpi.com/2079-9292/10/3/324.

[4] Pedro Bezerra and M.L. Heldwein. "Generation of hybrid carrier based modulation patterns". In: Oct. 2013, pp. 183–188. ISBN: 978-1-4799-0272-9. DOI: 10.1109/COBEP.2013.6785113.

[5] Ramulu Chinthamalla, K. Shivaji Ganesh, and Sachin Jain. "An optimal and efficient PV system using two 2-level cascaded 3-level inverter for Centrifugal pump". In: *2014 IEEE International Conference on Power Electronics, Drives and Energy Systems (PEDES)*. Dec. 2014, pp. 1–6. DOI: 10.1109/PEDES.2014.7042060.

[6] GreenMatch. *4 Reasons Behind the Rise of Renewables — GreenMatch*. en-GB. URL: https://www.greenmatch.co.uk/blog/2016/03/4-reasons-behind-the-rise-of-renewables (visited on 10/21/2021).

[7] Meng He. *SYNCHRONOUS OR NONSYNCHRONOUS TOPOLOGY? BOOST SYSTEM PERFORMANCE WITH THE RIGHT DC-DC CONVERTER*. en. publisher: Maxim Integrated. Jan. 2016. URL: https://www.maximintegrated.com/en/design/technical-documents/app-notes/6/6129.html (visited on 10/26/2021).

[8] Yap Hoon et al. "Control Algorithms of Shunt Active Power Filter for Harmonics Mitigation: A Review". en. In: *Energies* 10.12 (Dec. 2017), p. 2038. DOI: 10.3390/en10122038. URL: https://www.mdpi.com/1996-1073/10/12/2038 (visited on 10/26/2021).

[9] Nasir Hussein Selman. "Comparison Between Perturb & Observe, Incremental Conductance and Fuzzy Logic MPPT Techniques at Different Weather Conditions". In: *International Journal of Innovative Research in Science, Engineering and Technology* 5.7 (July 2016), pp. 12556–12569.

ISSN: 23476710, 23198753. DOI: 10.15680/IJIRSET.2016.0507069. URL: http://ijirset.com/upload/2016/july/69_Comparison.pdf (visited on 10/26/2021).

[10] Diodes Inc. *ZXGD3006E6(Rev. 6-2)*. https://www.diodes.com/assets/Datasheets/ZXGD3006E6.pdf. March 2018.

[11] Texas Instruments. *TMS320F2838x Real-Time Microcontrollers With Connectivity Manager TRM (Rev. D)*. https://www.ti.com/document-viewer/TMS320F28384D/datasheet. May 2019.

[12] A. Shukla, A. Ghosh, and A. Josh. "Flying capacitor multilevel inverter and its applications in series compensation of transmission lines". In: *IEEE Power Engineering Society General Meeting, 2004.* June 2004, 1453–1458 Vol.2. DOI: 10.1109/PES.2004.1373109.

[13] C. Sintamarean et al. "Wide-band gap devices in PV systems - opportunities and challenges". In: *2014 International Power Electronics Conference (IPEC-Hiroshima 2014 - ECCE ASIA)*. ISSN: 2150-6086. May 2014, pp. 1912–1919. DOI: 10.1109/IPEC.2014.6869846.

[14] Bineeta Soreng, Pradyumna Behera, and Raseswari Pradhan. "Design of A Grid Integrated PV System with MPPT Control and Voltage Oriented Controller using MATLAB/PLECES". In: *IOP Conference Series: Materials Science and Engineering* 225 (Aug. 2017), p. 012249. ISSN: 1757-8981, 1757-899X. DOI: 10.1088/1757-899X/225/1/012249. URL: https://iopscience.iop.org/article/10.1088/1757-899X/225/1/012249 (visited on 10/26/2021).

[15] Lei Tang et al. "One novel variable step-size MPPT algorithm for photovoltaic power generation". In: *IECON 2012 - 38th Annual Conference on IEEE Industrial Electronics Society*. ISSN: 1553-572X. Oct. 2012, pp. 5750–5755. DOI: 10.1109/IECON.2012.6389045.

[16] Wajahat Ullah Khan Tareen et al. "Mitigation of Power Quality Issues Due to High Penetration of Renewable Energy Sources in Electric Grid Systems Using Three-Phase APF/STATCOM Technologies: A Review". en. In: *Energies* 11.6 (June 2018), p. 1491. DOI: 10.3390/en11061491. URL: https://www.mdpi.com/1996-1073/11/6/1491 (visited on 10/26/2021).

[17] UnitedSiC. *UJ4C075033K3S(Rev. 2)*. https://www.mouser.com/ProductDetail/UnitedSiC/UJ4C075033K3S?qs=e8oIoAS2J1Rjf5BLB17IPg%3D%3D. July 2021.